The mechanism of the surface morphology transformation for the carbon nanotube thin film irradiated via excimer laser

Yun-Shan Chien, I-Che Lee, Po-Yu Yang, Chao-Lung Wang, Wan-Lin Tsai, Kuang-Yu Wang, Chia-Hsin Chou, and Huang-Chung Cheng

Citation: Applied Physics Letters **102**, 183111 (2013); doi: 10.1063/1.4804292
View online: http://dx.doi.org/10.1063/1.4804292
View Table of Contents: http://scitation.aip.org/content/aip/journal/apl/102/18?ver=pdfcov
Published by the AIP Publishing

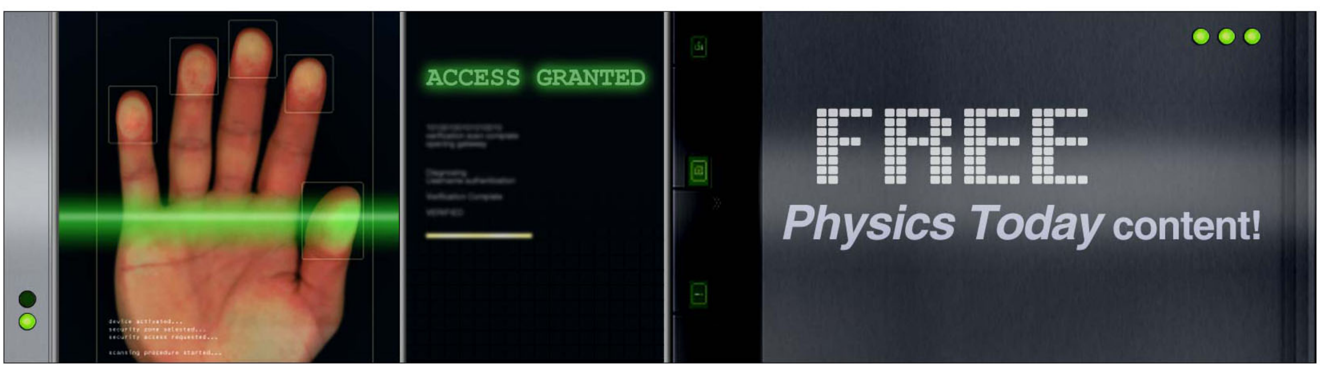

APPLIED PHYSICS LETTERS **102**, 183111 (2013)

The mechanism of the surface morphology transformation for the carbon nanotube thin film irradiated via excimer laser

Yun-Shan Chien,[a] I-Che Lee, Po-Yu Yang, Chao-Lung Wang, Wan-Lin Tsai, Kuang-Yu Wang, Chia-Hsin Chou, and Huang-Chung Cheng
Department of Electronics Engineering and Institute of Electronics, National Chiao Tung University, 1001 University Road, Hsinchu 300, Taiwan

(Received 18 March 2013; accepted 24 April 2013; published online 8 May 2013)

In this paper, the surface morphology transformation of the sprayed carbon nanotube (CNT) thin film irradiated with the excimer laser has been systematically investigated. Under the excimer-laser irradiation, two phenomena, including the annealing and ablation effects, were found to be dependent on the incident laser energy and overlapping ratios. Moreover, the extremely high protrusions would be produced in the interface between the annealing and ablation regions. The mechanism of the CNT thin film under the excimer laser irradiation was, therefore, proposed to derive the surface morphology modifications and the further reinforced crystallinity with proper laser energy densities and overlapping ratios. © *2013 AIP Publishing LLC*.
[http://dx.doi.org/10.1063/1.4804292]

Carbon nanotubes (CNTs) were considered as one of future potential alternates for being applied in the sensors[1,2] and optoelectronic devices,[3,4] owing to the unique high-aspect-ratio structures, chemical, and physical properties. Recently, a process to synthesize two-dimensional (2D) CNT thin film[5,6] with good electrical, chemical, and mechanical properties had been developed to overcome the high growth temperature. In order to improve chemical and physical properties of CNT thin film, plasma bombardment, high temperature thermal annealing, and laser irradiation as post treatments have been proposed. Among these post treatments, the thermal annealing and laser irradiation were conducted to improve the electrical and physical properties. Although the thermal annealing could achieve improvements in both chemical and electrical characteristics,[7] the high temperature propose limited the choices of substrates to expensive quartz or silicon substrates. Consequently, the excimer-laser irradiation[8,9] has attracted more attention on the treatment for the CNT thin film on glass or plastic substrates due to low temperature process. Furthermore, the laser irradiation could also be applied to the etching and lithography process for obtaining surface morphology variations.[10,11] However, excimer laser irradiation effects on the surface morphology transformation of the CNT thin film were not yet discussed clearly. Therefore, a mechanism was proposed to explain the surface morphology transformation of the sprayed CNT thin film under excimer laser irradiation with various laser energy densities and overlapping ratios.

First, the thermal chemical-vapour-deposition grown CNTs were chemically treated by the H_2SO_4/HNO_3 oxidation solution, followed by ultrasonicating and centrifugating to obtain a homogeneous CNT solution. Then, the derived CNT solution was ultrasonically sprayed onto the wet-oxidized silicon substrates to form a continuous CNT network. Subsequently, such a CNT thin film was irradiated with the KrF laser ($\lambda = 248$ nm) in a vacuum chamber pumped down to 2×10^{-2} Torr at room temperature. The laser beam size was 2 mm in width and 20 mm in length, and the pulse duration was 23 ns with the maximum repetition frequency of 10 Hz. The KrF excimer laser was a semi-Gaussian beam profile, and the energy distribution was nearly uniform across the 20 mm in length with the direction perpendicular to the scanning path. The excimer laser energy densities were ranged from 20 mJ/cm^2 to 400 mJ/cm^2, and the irradiation shots were varied from 1 shot to 100 shots, i.e., 0% to 99% overlapping ratios. The 1-shot irradiation, namely the single-scan condition, is corresponding to the 0% overlapping ratio. As for the 100-shots condition, the scanned laser beam and the next one were overlapped with overlapping ratio of 99%. The surface morphologies were then observed by field-emission scanning electron microscopy (FE-SEM; Hitachi S-4700I) and optical microscopy (OM). The crystallinity was examined by the Raman spectrum (HOROBA; Lab RAM HR) and X-ray photoelectron spectroscopy (XPS; Physical Electronics PHI-1600).

Fig. 1 illuminates the OM and FE-SEM images of the single-scanned CNT thin films irradiated at various energy densities. For the single-scan condition, Figs. 1(a) and 1(d) show the OM and FE-SEM images of CNT thin films annealed at 20 mJ/cm^2, respectively, and the surface morphology was observed to remain unchanged. At the higher applied energy density of 100 mJ/cm^2, part of the CNT thin film was ablated, peeled, and accompanied with the formation of the CNT protrusions at the edge of the ablation area, as shown in Figs. 1(b) and 1(e). Once the CNT thin film started to ablate and accompany with surface protrusions, the laser energy was defined as ablation energy. For as-sprayed CNT thin film, the ablation energy was measured to be about 99 mJ/cm^2. As the laser energy density was elevated to 160 mJ/cm^2, the ablation region was apparently widened, as shown in Figs. 1(c) and 1(f), because the nearby CNT thin film was eradicated simultaneously. In order to realize the laser-irradiated overlapping effects, multiple-scan conditions were applied on the CNT thin film. For the 95% overlapping, i.e., 20 shots, the CNT thin film surface morphology still

[a]Author to whom correspondence should be addressed. Electronic mail: u930347@oz.nthu.edu.tw

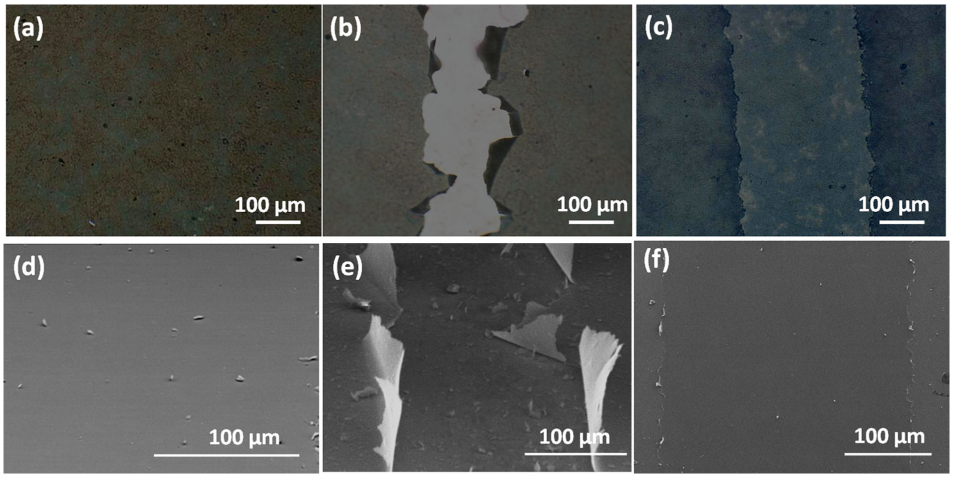

FIG. 1. The optical microscopy images of the single-scanned CNT thin films irradiated with (a) 20 mJ/cm^2, (b) 100 mJ/cm^2, and (c) 160 mJ/cm^2, respectively. The FE-SEM images of the single-scanned CNT ones annealed at (d) 20 mJ/cm^2, (e) 100 mJ/cm^2, and (f) 160 mJ/cm^2, accordingly.

remained uniform without any variation as the laser energy density at 100 mJ/cm^2, as shown in Fig. 2(a). As compared with single-scan condition, the CNT thin film seems more robust against the laser irradiation for the multiple-scan one. As the laser energy was raised to 220 mJ/cm^2, the surface protrusions accompanied with simultaneous ablation began to occur in the surface of irradiated CNT thin film, as demonstrated in Fig. 2(b). For the multiple-scan one with the laser energy to 240 mJ/cm^2, the ablation area became wider and the surface protrusions were more vertical, as displayed in Fig. 2(c). Furthermore, as the laser energy was further increased to 280 mJ/cm^2, most of CNT thin film was directly ablated, as displayed in Fig. 2(d). As compared with single-scan condition, it was found that the energy density needed to ablate the CNT thin film was elevated for the overlapping conditions.

To realize the crystallinity change after the laser irradiation, the Raman spectrum was conducted to examine the CNT thin film under various laser energy densities for the 95% overlapping, as demonstrated in Fig. 3(a). Two main peaks of Raman shifts were observed, G peak (1584 cm^{-1}) and D peak (1322 cm^{-1}), respectively. The G peak was ascribed to the graphite E_{2g} and sp^2-bond vibration mode, while the D peak was originated from the crystal defects, dangling bonds, and amorphous carbon.[12,13] The ratio of I_D/I_G was calculated from the intensity division of D band and G band. For the as-sprayed CNT thin film, the I_D/I_G ratio was calculated to be 2.03. It reflected that the structures of CNTs after acid oxidation were destroyed seriously, and C-C bonding was connected with the functional groups.[2] After the laser irradiation, the I_D/I_G ratio was remarkably decreased to 1.203 for the laser irradiated ones with the laser energy density at 240 mJ/cm^2. The reduced I_D/I_G ratio suggested the crystallinity improvement after laser irradiation. Moreover, the degree of graphitization could be characterized by the intensity ratio of $I_G/(I_D + I_G)$, and the higher $I_G/(I_D + I_G)$ ratio represented the higher degree of graphitization.[14] The $I_G/(I_D + I_G)$ ratio increased from 0.3485 to 0.4613 after excimer laser irradiation. The Raman results implied that the high laser energy irradiation would lead to graphitization of the CNT thin film.[4] However, the overhigh energy at 260 mJ/cm^2 would directly ablate and destroy the structures of CNT thin films, resulting in the increased I_D/I_G ratio.[15] The XPS analyses of the as-sprayed and excimer-laser-irradiated CNT thin film were also performed to approve such results, as shown in Figs. 3(b) and 3(c). For the as-sprayed CNT thin film, the main C1s spectrum could be identified into C=C sp^2 bonds (284.2 eV), C-O bonds (285.8 eV), and C=O bonds (288.8 eV), and the functional groups mainly originated from the oxidation.[2] After laser irradiation, the intensity of C-O and C=O bonds was notably reduced. Furthermore, there was a new peak appearance around 290 eV, which was assigned to the π-π* transition.[16] The results also demonstrate the graphitization occurrence under the laser irradiation.

For depicting the excimer laser irradiation effects on the CNT thin film, a schematic illustration has been proposed in Fig. 4. The excimer laser energy profile was corresponding to the Gaussian distribution crossing the 2 mm width, as demonstrated in Fig. 4(a). For the single-scan irradiation, there existed three different surface morphology regions, ablation, protrusions, and no variations, corresponding to the irradiated regions with the highest, medium, and lowest energy densities, accordingly. As the laser energy exceeded ablation energy, the irradiated region would be directly ablated, named as the ablation region. As the laser energy was lower than ablation energy, the CNT thin film was just annealed and the morphology of surface remained

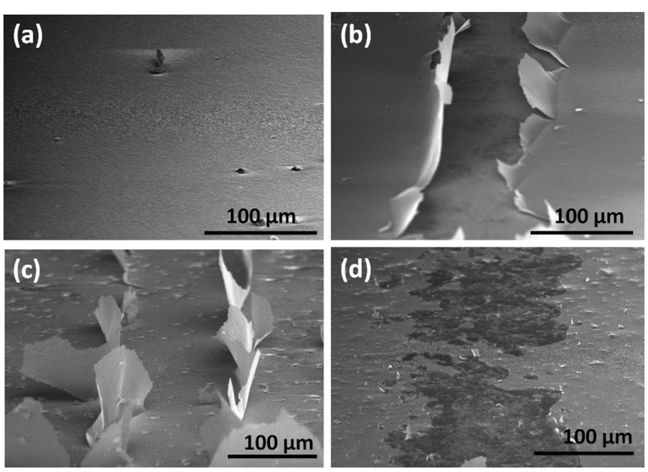

FIG. 2. The FE-SEM images of the multiple-scan condition for 95% overlapping with (a) 100 mJ/cm^2, (b) 220 mJ/cm^2, (c) 240 mJ/cm^2, and (d) 280 mJ/cm^2, accordingly.

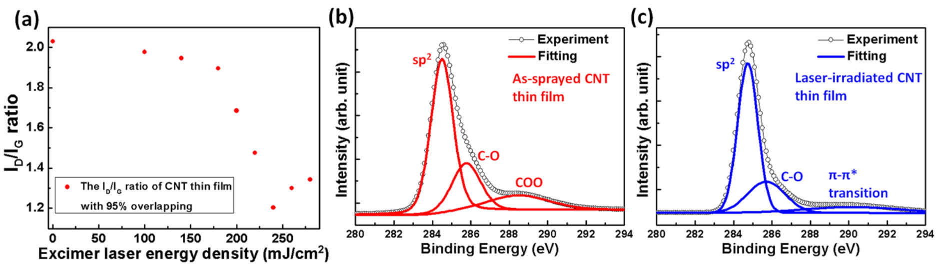

FIG. 3. (a) The Raman spectrum of the excimer-laser irradiated CNT thin films with various laser energy densities for the 95% overlapping. The XPS analyses of (b) the as-sprayed CNT thin film and (c) the excimer-laser irradiated CNT thin film.

unchanged, called as the annealing region. Furthermore, there existed surface protrusions at the interfaces between the ablation and annealing regions. It was reported that the surface protrusions occurred as the CNTs were ablated under the high energy laser irradiation.[17] For the multiple-scan conditions, the ablation energy of CNT thin film would increase to a higher value than the single-scan condition, since the continued irradiation would enhance the crystallinity of CNT thin film. Owing to the increased ablation energy, the reduced ablation region of multiple-scan with respect to single-scan one under the same laser annealing energy was demonstrated in Fig. 4(b).

Furthermore, the multiple-scan effects of the excimer-laser irradiated CNT thin film were investigated via the relationship between the laser annealing and ablation energy densities. Fig. 5 demonstrates the ablation energy as the functions of the annealing energy under different overlapping ratios, i.e., various scanning shots. For the single-scan condition, the energy needed to ablate CNTs was almost the same as 99 mJ/cm^2, according to the calculation from Fig. 1(b). As for the 90% overlapping irradiation, the ablation energy would be raised to 118 mJ/cm^2 for the 60 mJ/cm^2 annealing, and the ablation energy was increased to 342 mJ/cm^2 for the 280 mJ/cm^2 annealing. Moreover, the ablation energy would be further increased to be 360 mJ/cm^2 and 387 mJ/cm^2 for the 95% and 99% overlapping annealing under the 280 mJ/cm^2 annealing, respectively. It implied that the elevated annealing energy could promote the crystallinity of CNT thin film, leading to the increased ablation energy. With the 99% overlapping, the ablation energy was observed to saturate under high energy annealing. This phenomenon implied that the crystallinity of CNT thin film would be enhanced rapidly under low laser energy. The photon energy of KrF excimer energy (5.0 eV) was high enough to break the weak sp^3 bonds such as C-H (1.41–1.61 eV),[18] C-O (2.44–2.48 eV),[19] and C-C (3.175–4.983 eV),[20] which originated from the chemical oxidation.[2] However, under the high laser energy annealing, the continuous laser beam irradiation caused the surface local heating, which was not sufficient for the underneath part C-C bonds rearranging.

Although the first irradiated scan on the CNT thin film would cause the ablation in the region corresponding to energy above 99 mJ/cm^2, the ablation energy of the remained CNT thin film was simultaneously increased to resist the next scanned laser beam. The continuous irradiation on the CNT thin film, therefore, increased the ablation energy. Consequently, the increased annealing energy and overlapping shots assisted the reinforced crystalline structures, resulting in the elevated ablation energy. Therefore, the ablation energy densities could be estimated, and the surface morphologies could be precisely obtained for different irradiation conditions.

In summary, the transformation of CNT thin film surface morphologies via excimer laser irradiation under various laser energies and overlapping ratios was systematically investigated. For the single-scan condition, there existed

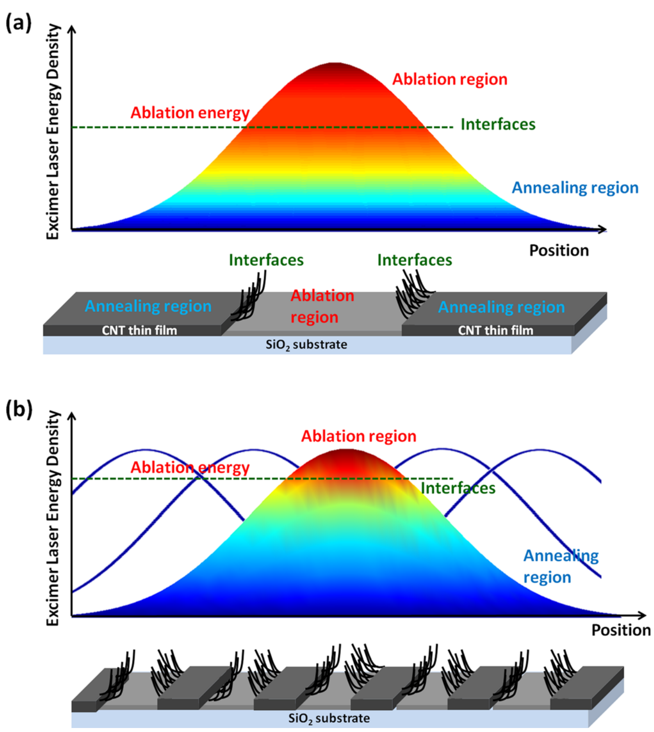

FIG. 4. (a) The laser energy profile of the single-scan condition for the CNT thin film surface morphology transformation. (b) The laser energy profile of the multiple-scan condition for the CNT thin film surface morphology transformation.

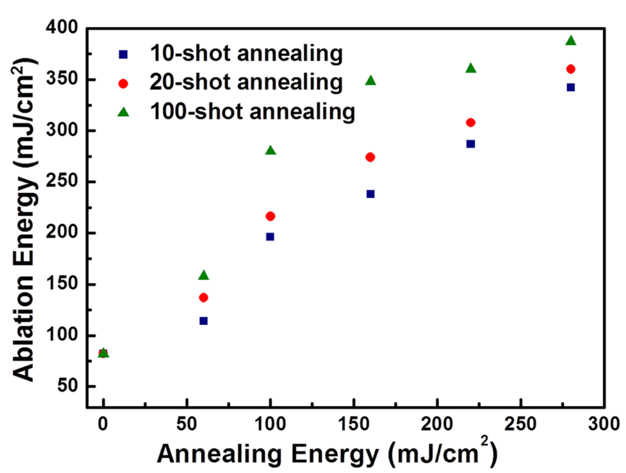

FIG. 5. The ablation energy varies with the annealing energy under 90%, 95%, and 99% overlapping, respectively.

three different surface morphology regions, ablation, protrusions, and no variations, corresponding to the irradiated regions with the highest, medium, and lowest energy densities, accordingly. The increased shots for the multiple-scan condition would be favorable for the improvement of CNT crystallinity, resulting in the higher ablation energy. Furthermore, the elevated annealing energy would as well as increase with the ablation energy. Therefore, the surface morphology and the crystallinity of CNT thin film could be accurately obtained by various excimer laser irradiated conditions.

This work was supported by the National Science Council of the Republic of China under the Grant No. NSC 101-2221-E-009-077-MY3, and in part by the Nano Facility Center of National Chiao Tung University, and National Nano Device Laboratories (NDL) for providing process equipment.

[1]J. H. Kwon, K. S. Lee, Y. H. Lee, and B. K. Ju, Electrochem. Solid-State Lett. **9**, H85 (2006).
[2]Y. S. Chien, W. L. Tsai, I. C. Lee, J. C. Chou, and H. C. Cheng, IEEE Electron Device Lett. **33**, 1622 (2012).
[3]K. J. Chen, W. K. Hong, C. P. Lin, K. H. Chen, L. C. Chen, and H. C. Cheng, Jpn. J. Appl. Phys., Part 1 **41**, 6132 (2002).
[4]K. F. Chen, K. C. Chen, Y. C. Jiang, L. Y. Jiang, Y. Y. Chang, M. C. Hsiao, and L. H. Chan, Appl. Phys. Lett. **88**, 193127 (2006).
[5]Y. Zhou, L. Hu, and G. Grüner, Appl. Phys. Lett. **88**, 123109 (2006).
[6]Y. Feng, X. Ju, W. Feng, H. Zhang, Y. Cheng, J. Liu, A. Fujii, M. Ozaki, and K. Yoshin, Appl. Phys. Lett. **94**, 123302 (2009).
[7]J. Zhang, C. Yang, Y. Wang, T. Feng, W. Yu, J. Jiang, X. Wang, and X. Liu, Nanotechnology **17**, 257 (2006).
[8]H. Huang, R. Maruyama, K. Noda, H. Kajiura, and K. Kadono, J. Phys. Chem. B **110**, 7316 (2006).
[9]T. Honda, C. B. Oh, K. Murakami, W. S. Kim, S. Abo, F. Wakaya, and M. Takai, J. Vac. Sci. Technol. B **24**, 1013 (2006).
[10]A. Lasagni, R. Cross, S. Graham, and S. Das, Nanotechnology **20**, 245305 (2009).
[11]H. K. Lin, R. C. Lin, and C. H. Li, Thin Solid Films **518**, 7253 (2010).
[12]P. C. Eklund, J. M. Holden, and R. A. Jishi, Carbon **33**, 959 (1995).
[13]M. Sveningsson, R.-E. Morjan, O. A. Nerushev, Y. Sato, J. Bäckström, E. E. B. Campbell, and F. Rohmund, Appl. Phys. A: Mater. Sci. Process. **73**, 409 (2001).
[14]J. H. Ting, T. L. Li, and Y. C. Hong, J. Vac. Sci. Technol. B **24**, 1794 (2006).
[15]Á. P. d. Pino, E. György, L. Cabana, B. Ballesteros, and G. Tobias, Carbon **50**, 4450 (2012).
[16]Z. R. Ismagilov, A. E. Shalagina, O. Y. Podyacheva, A. V. Ischenko, L. S. Kibis, A. V. Boronin, Y. A. Chesalov, D. I. Kochubey, A. I. Romanenko, O. B. Anikeeva, T. I. Buryakov, and E. N. Tkachev, Carbon **47**, 1922 (2009).
[17]K. Ohsumi, T. Honda, W. S. Kim, C. B. Oh, K. Murakami, S. Abo, F. Wakaya, M. Takai, S. Nakata, A. Hosono, and S. Okuda, J. Vac. Sci. Technol. B **25**, 557 (2007).
[18]D. Jiang, B. G. Sumpter, and S. Dai, J. Chem. Phys. **126**, 134701 (2007).
[19]X. Y. Zhu, S. M. Lee, Y. H. Lee, and T. Frauenheim, Phys. Rev. Lett. **85**, 2757 (2000).
[20]S. Dag, O. Gülseren, T. Yildirim, and S. Ciraci, Phys. Rev. B **67**, 165424 (2003).